

A transformative approach to ageing fish otoliths using Fourier transform near infrared spectroscopy: a case study of eastern Bering Sea walleye pollock (*Gadus chalcogrammus*)

Thomas E. Helser, Irina Benson, Jason Erickson, Jordan Healy, Craig Kastle, and Jonathan A. Short

Abstract: We investigated the use of Fourier transform near infrared spectroscopy (FT-NIRS), which is a method of measuring light absorbance signatures, to derive ages from eastern Bering Sea walleye pollock (*Gadus chalcogrammus*) otoliths. This approach is based on a predictive model between near infrared spectra in the otolith and fish age, which is calibrated and validated. The advantage of FT-NIRS over traditional methods is the speed and repeatability with which age estimates are generated. The application of FT-NIRS to walleye pollock otoliths yielded r^2 values between 0.91 and 0.95 for the calibration models and good validation performance (between 0.82 and 0.93). This approach can be expected to predict fish age within ± 1.0 year of age 67% of the time. When comparing approaches, the FT-NIRS had as good or slightly better precision (75% agreement) than the traditional ageing (66% agreement) and showed little or no bias at age before 12 years of age. Once the predictive FT-NIR model is calibrated and validated, age estimates using FT-NIRS can be done at 10 times the rate compared to traditional methods.

Résumé : Nous avons examiné l'utilisation de la spectroscopie dans le proche infrarouge par transformation de Fourier (SPIR-TF), une méthode pour mesurer les signatures d'absorbance de la lumière, pour obtenir des âges à partir d'otolithes de goberges de l'Alaska (*Gadus chalcogrammus*) de la mer de Behring orientale. Cette approche est basée sur un modèle prédictif reliant des spectres de proche infrarouge d'otolithes et l'âge des poissons, qui est étalonné et validé. L'avantage de la SPIR-TF par rapport aux méthodes traditionnelles est la vitesse et la répétabilité avec lesquelles les estimations des âges sont produites. Pour l'application de la SPIR-TF au goberge de l'Alaska, les otolithes ont donné des valeurs de r^2 de 0,91 à 0,95 pour les modèles d'étalonnage et une bonne performance en ce qui concerne la validation (de 0,82 à 0,93). Cette approche devrait pouvoir prédire l'âge de poissons à $\pm 1,0$ an après 67 % du temps. La comparaison des approches fait ressortir le fait que la SPIR-TF produit une bonne précision ou une précision légèrement meilleure (75 % de concordance) que la méthode traditionnelle de détermination de l'âge (66 % de concordance) et présente peu ou pas de biais pour un âge donné avant l'âge de 12 ans. Une fois le modèle PIR-TF étalonné et validé, des estimations de l'âge faisant appel à la SPIR-TF peuvent être obtenues à un rythme 10 fois supérieur à celui des méthodes traditionnelles. [Traduit par la Rédaction]

Introduction

Fish ages are one of the fundamental data elements of integrated stock assessments because they provide information on recruitment, growth, maturity, and production (Maunder and Punt 2013; Ono et al. 2015). Estimation of age composition, size at age, maturity at age, and longevity of a fish population is critical for assessing the overfishing or overfished status of a stock (Ricker 1975; Hilborn and Walters 1992; Campana and Thorrold 2001; Chen et al. 2003; Conn et al. 2010; Coggins et al. 2013; Maunder and Punt 2013; Ono et al. 2015). Fish age has historically been determined by microscopically counting pairs of annual opaque and translucent growth zones in a number of different hard structures including scales, vertebrae, opercula, spines, and most commonly otoliths (Bagenal and Tesch 1978; Chilton and Beamish 1982).

In federally managed waters of the United States, over 1.1 million hard structures (minimum estimate) have been examined for age estimates during the period from 2008 to 2015 (T.E. Helser, personal communication) and most management regions have shown a steady increase in the number of otoliths aged per year. In the federally managed waters of Alaska, 633 000 otoliths were

collected from research surveys and commercial fisheries during the last 9 years, from which over 352 000 fish ages were estimated and used in assessment models to support of scientific advice to the North Pacific Fishery Management Council (T.E. Helser, personal communication). While most population assessment models employ age data, depending on species and complexity of the model, the most dramatic cases are eastern Bering Sea (EBS) and Gulf of Alaska walleye pollock (*Gadus chalcogrammus*) with over 12 000 ages annually followed by Pacific cod (*Gadus macrocephalus*) with over 3300 annually. The EBS walleye pollock supports the most valuable fishery in Alaska with the Bering Sea and Aleutian Islands pollock first-wholesale value accounting for \$1.35 billion in 2016, \$1.27 billion in 2015, and an average of \$1.25 billion in 2005–2007 (Ianneli et al. 2017). Other species in federally managed waters of Alaska account for the remaining total of otoliths aged, which has an average of about 20 000-year⁻¹ (T.E. Helser, personal communication).

A large investment is made in the age determination and production process of age data to support stock assessments. While the traditional production approach varies in the procedures used

Received 20 March 2018. Accepted 12 July 2018.

T.E. Helser, I. Benson, C. Kastle, and J.A. Short. Resource Ecology and Fisheries Management Division, Alaska Fisheries Science Center, National Marine Fisheries Service, NOAA, 7600 Sand Point Way NE, Seattle, WA 98115, USA.

J. Erickson. Bruker Optics, Inc., 40 Manning Road, Billerica, MA 01821, USA.

J. Healy. University of Washington, School of Aquatic and Fisheries Science, 1122 NE Boat Street, Seattle, WA 98195, USA.

Corresponding author: Thomas E. Helser (email: thomas.helser@noaa.gov).

Copyright remains with the author(s) or their institution(s). Permission for reuse (free in most cases) can be obtained from [RightsLink](https://www.rightslink.com).

to prepare and count the number of growth zones in the otoliths depending on species, the hard structures require some degree of handling time in the process of embedding, sectioning, cutting, and burning to enhance growth zones and microscopic examination. Otoliths are processed and aged using a variety of methods including surface reading, breaking the otolith transversely and either baking it or burning the edge, and thin sectioning. The breaking and thin sectioning methods expose annuli that form on the proximal side of the otolith, which are not visible by surface reading (Beamish and McFarlane 1995). Each method has its advantages and shortcomings in terms of associated costs and quantity and quality of outputs (Begg et al. 2005). For instance, an analysis of 10 years of age production data from the Alaska Fisheries Science Center (AFSC) showed that the rate of output depended on the maximum age of the species, method of processing, and the age reading difficulty (T.E. Helsler, personal communication). Comparatively, there was more than a 50% reduction in efficiency for a long-lived rockfish that required sectioning, such as Pacific Ocean perch (*Sebastes alutus*), versus a short-lived groundfish, such as walleye pollock, where age can be estimated by a combination of surface and break-and-burn techniques. Hence, when considering the time from when the otolith is collected at sea to the time a trained expert age reader produces an age estimate, quite an investment has gone into the generation of a single age. Age data have been referred to as one of the most expensive sources of data collected for stock assessments (Campana 1999). Furthermore, most production ageing laboratories employ quality control procedures (to estimate precision and bias) where some percentage (usually between 10% and 20%) of the total specimens are handled and read a second time by another independent expert age reader to estimate age reading precision (Kimura and Anderl 2005). This is a crucial stage in the process because ignoring ageing error can lead to bias in estimates of growth, masses, or maturity at age and estimates of natural mortality by affecting the estimate of productivity (i.e., less older fish means higher natural mortality and higher productivity). Hence, ageing error can in turn affect management indicators or reference points (Reeves 2003; De Pontual et al. 2006; Bertignac and De Pontual 2007).

It is widely accepted that age determination of hard-part structures requires some degree of subjectivity. Different analysts can examine the same structure microscopically and interpret and produce different age estimates. There are two aspects to ageing error: precision and accuracy (Beamish and McFarlane 1995). Precision reflects the repeatability of age estimates on one specimen from one age reader to another. It can be expressed as percent agreement (PA) between independent readers, average percent error (APE), or coefficient of variation (CV), the two latter being functionally equivalent, although reporting the CV has been favored in some studies (Beamish and Fournier 1981; Chang 1982; Campana and Thorrold 2001). Precision is an aspect of the ageing error that will always occur, as it is inherent to the nature of the structure and species being assessed (Beamish and McFarlane 1995; Campana and Thorrold 2001). Accuracy is the relationship between estimated and true age (Beamish and McFarlane 1995); that is, it is an estimation of bias. It is often estimated by age validation methods (e.g., bomb radiocarbon, mark-recapture, marginal increment analysis, etc.) (see review in Campana and Thorrold 2001).

Efforts to streamline, increase the efficiency, and improve repeatability of age determination have been the focus of a number machine-based technologies during the last several decades. Historically, machine-based or computerized fish age determination has been attempted with various levels of success using otolith morphometrics (Pilling et al. 2007; Fablet et al. 2009; Mahe et al. 2016), image analysis (Nasreddine et al. 2013), or both (Troade and Benzinou 2002; Fablet and Le Josse 2005). When a large number of fish need to be aged, such as for stock assessments, the goal may be to produce fish ages more efficiently while not hindering age

accuracy or precision (Fablet and Le Josse 2005). While a number of alternative approaches have been explored for use in age estimation, few if any have assisted experts trained in otolith interpretation and none have been developed as a large-scale production age determination tool. Recently, new applications in the established technology of Fourier transform near infrared spectroscopy (FT-NIRS) have been applied to fish otoliths (Wedding et al. 2014; Robins et al. 2015) and shark vertebrae (Rigby et al. 2016) for age determination. FT-NIRS is used in a wide variety of industries including pharmaceutical, chemical, petrochemical, agricultural and food, and feed and dairy manufacturing. FT-NIRS is capable of providing both qualitative and quantitative information about the material or product being analyzed. It has applications ranging from raw material identification to quality control monitoring and determination of product composition. FT-NIRS itself is a vibrational spectroscopy technique based on the interaction of electromagnetic energy of a specific frequency range with the covalent bonds in organic molecules. The bonds associated with different functional groups (C–H, N–H, and O–H) absorb energy at unique and characteristic frequencies, and the relative amount of each functional group present is proportional to the amount of energy absorbed. This relationship is what allows this technique to be utilized for quantitative analytical work.

Why does NIRS work on fish otoliths? Fish otoliths are composed of >90% calcium carbonate (CaCO_3), 3%–4% organic matrix (protein called otolin), and about 1% inorganic trace elements (Campana 1999). While morphological properties (size, mass, and growth) and chemical composition vary widely among fish species (Zorica et al. 2010), the quantity of protein in the calcium carbonate matrix accumulates as fish grow older. NIRS quantitatively measures the absorption of near infrared energy by the protein molecules. Specifically, when the protein molecules are irradiated by a source of near infrared energy, they absorb some of this energy at specific frequencies that correspond to the vibrational frequency of the bonds in the protein molecules. An instrument known as an FT-NIR spectrometer provides the energy source, scans the object, and measures and records this interaction in the form of a near infrared “spectrum” of the material. The spectral regions most meaningful for otoliths are the regions corresponding to the molecular constituents in proteins such as C–H, O–H, and N–H groups. As such, the chemical properties of the otoliths provide the spectral information and the quantity of the absorbed NIR energy within those specific regions is a proxy for fish age. Analyses of saddletail snapper (*Lutjanus malabaricus*) in Australia found that NIRS predictive models could predict the age of fish from otoliths with a high degree of accuracy, leading to reduced costs per sample and reduced subjectivity (Wedding et al. 2014). In fisheries science, the application of FT-NIR spectroscopy to age fish is quite novel and so far has been tested on a very limited number of species.

The objective of this study was to test the use of FT-NIRS to age EBS walleye pollock. This involved (1) collecting spectral scans of walleye pollock otoliths, (2) using spectral data to calibrate and validate a model that predicts ages relative to traditional age estimation methods, (3) explore spatial and temporal stability in the calibration-validation models, and (4) compare the relative accuracy and precision between ages generated between the FT-NIRS and “traditional” production procedures.

Materials and methods

For this study, walleye pollock otoliths along with biological and station location data were taken from the AFSC’s 2016 and 2017 EBS shelf bottom trawl survey (BTS). The EBS BTS is conducted annually using a 20 nautical mile fixed-grid design stratified by depths corresponding to inner (0–50 m), middle (50–100 m), and outer (>100 m) domains and further subdivided into southeast to northwest strata. The standard survey area encompasses 492 898 km²

and annually averages approximately 350 hauls, each made at the center of a grid cell. Details of the EBS BTS design and catch sampling can be found in [Conner and Lauth \(2017\)](#) and [Stauffer \(2004\)](#). Sampling for walleye pollock otoliths was random within each haul. The survey area was divided into low- and high-density strata based on historical density and an isobath of approximately 70 m. Otoliths were collected from all hauls in which the total number of walleye pollock was greater than 19. Five pairs of otoliths were collected in high-density strata and three in low-density strata. Approximately 1700 walleye pollock otolith pairs were collected in each year and transported to the AFSC's Age & Growth Laboratory for analysis.

To facilitate exploration of spatial variability, we conducted a statistical spatial analysis to stratify the EBS survey area into distinct regions based on fish growth and morphometrics. Since geographic regions with differing water temperatures, depths, and growth are thought to influence biomineralization ([Chang and Geffen 2013](#)) in otoliths, we sought to stratify using an objective measure readily available in the data. In particular, walleye pollock condition indices ([Ricker 1975](#)) were calculated from individual length and mass data and analyzed using the Getis–Ord ([Getis and Ord 1992](#)) statistic, which measures the concentration or lack of concentration (referred to as “hotspots”) in a spatially ordered variable.

Otolith samples and age determination

Prediction of fish age from FT-NIRS spectral data requires development of a “model calibration” or “training” set that encompasses the full range of ages, spectral variation (space and time), and instrument measurement conditions. Here the goal is to ensure that the calibration model is robust and minimizes extrapolation outside the boundaries of the reference data. A second “external validation” set is also chosen to test the predictive model. Details of walleye pollock age determination can be found in [Matta and Kimura \(2012\)](#); however, a brief explanation is provided here related to processing otoliths for both age and spectral data. For age determination, walleye pollock sagittal otoliths are first cut in the transverse plane using a low-speed saw and then roasted in either an oven or alcohol flame to enhance growth patterns. Age is estimated by counting the consecutive pairs of opaque and translucent zones corresponding to the summer and winter growths zones, respectively. A 20% random subsample (test set) of the total AFSC's annual collection is independently aged a second time by an expert analyst for calculating precision and bias (relative) statistics associated with the age determination process. For the 2016 and 2017 test data, we computed PA, APE ([Beamish and Fournier 1981](#)), and the CV ([Chang 1982](#)) to evaluate interreader precision for a given sample. High PA values and low CV and APE (<5.0) values indicate good precision between age estimates. All precision statistics are relayed to data end users at the AFSC. For collection of spectral data (both calibration and validation sets), we used the unroasted sagittal otoliths from among the AFSC test set so as to provide the best possible reference ages (i.e., evaluated by two independent analysts).

We employed two different sampling procedures for the 2016 and 2017 survey otolith collections to partition the calibration and validation data sets. For the 2016 calibration set, otoliths were selected on the basis of a uniform sampling distribution on age, giving about 10 samples per each age group (ages 1–12+). This ensured that sparse samples on the extremes of the age distribution are represented in the calibration. The external validation collection, which consisted of about 66% more otoliths, was taken as a random selection of the entire 2016 collection. For 2017, the test set of 20% of otoliths from the entire AFSC's 2017 collection was used for spectral data acquisition and the calibration and external validation sets were equal in number.

Spectral data acquisition and pretreatment

Spectral data from all otoliths were collected on a Bruker TANGO-R FT-NIR spectrometer, which is a dedicated single-channel spectrometer for diffuse reflectance measurements. Otoliths were placed on the spherical quartz sampling window distal side up and scanned at three separate orientations relating to 0°, 45°, and 90° positions. A gold-coated reflector was placed over the otolith to capture any “stray” light due to the irregular shape of the otolith as compared to the sampling window. Data were acquired at 16 cm⁻¹ resolution with 64 co-added scans (which were averaged into a final raw absorbance spectrum) for each otolith position, resulting in three separate spectra for each specimen. Here we wanted to analyze the variation in the spectral information associated with an unstandardized orientation of the otolith position. Statistical tests were performed by analysis of covariance of FT-NIR age estimates on reference age with position as a class variable.

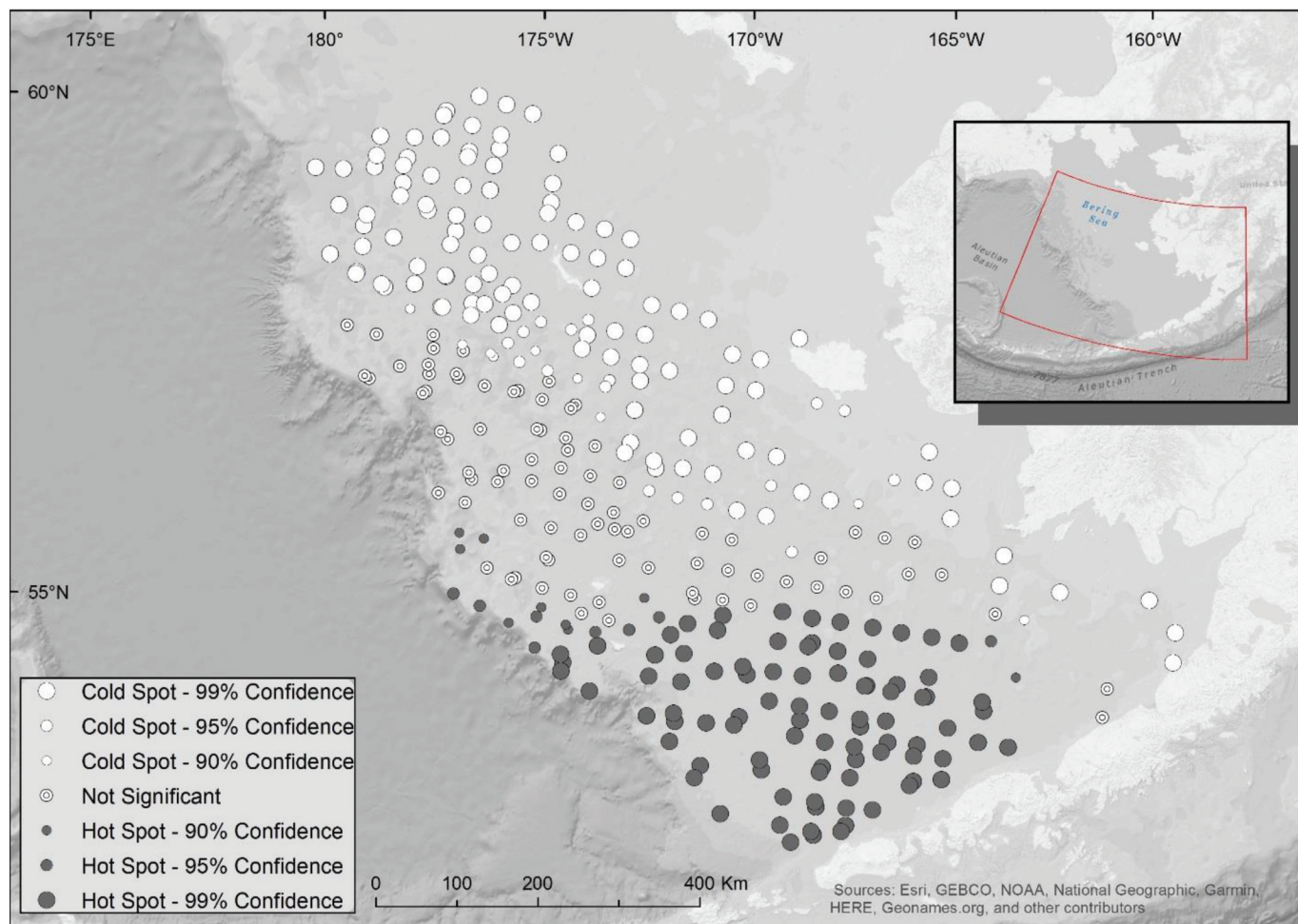
Once all spectral data were acquired, we used the chemometric software package OPUS (version 7.8, Bruker Optics) for data processing and model generation. The software allows for multiple combinations of spectral regions and data preprocessing techniques to be considered and then the optimal model can be selected. It was found that application of a first-derivative (17-point Savitsky–Golay smooth) transformation to the spectral data (which removes slope in the baseline and enhances subtle spectral variation) yielded the best models.

FT-NIRS calibration and validation

We used partial least squares (PLS) regression ([Chen and Wang 2001](#)), which is a multivariate calibration method, to develop a quantitative NIR model to predict age. In PLS, the information contained in the spectral data (the X data matrix) is compared to reference values for the component of interest (the Y data matrix) and changes that occur in both matrices are correlated with each other. Following any pretreatment steps, the spectral data are broken down into principal components or factors (also called loadings) and scores, which allows the most relevant spectral information to be retained while the “noise” or nonrelevant information in the data can be disregarded. Furthermore, spectral regions with the highest correlation with changes in the reference values can be identified and isolated. Evaluation of the loadings and regression coefficients is used to determine the optimal number of factors (or rank) to include in the model without “overfitting” the data.

Practically speaking, a set of representative samples (the calibration samples) are measured with an NIR spectrometer to obtain the NIR spectra and the corresponding reference values (in this case age) are determined (in this case by the reader). The spectral data and corresponding reference values are input into the chemometric software package and the model is generated. This is done using the process of “cross validation” where each calibration sample is temporarily removed from the data set, a PLS model is created from the remaining samples, and the sample that was temporarily removed is predicted as an unknown. The difference between the reference value and the predicted value is determined and the sample is returned to the data set. This process is repeated until each sample has been removed once. The mean error of prediction for the temporarily removed unknowns is calculated as the root mean square error of cross validation, or RMSECV, and is an indication of the model accuracy. Once a cross-validated model was obtained, we further assessed the performance (robustness) of this model by using the model to predict a completely new set of representative unknown samples. This process is called “external” validation. In this case, the entire test set is predicted by the model and the residual (NIR prediction versus reference value) for each sample is calculated. The mean error of prediction for the external validation set is calculated as the root mean square error of prediction (RMSEP). For a robust model, the

Fig. 1. Spatial statistical analysis using Getis–Ord (Getis and Ord 1992) statistic, which measures the relative concentration (referred to as “hotspots”) in a spatially ordered variable. Here, walleye pollock (*Gadus chalcogrammus*) fish condition is used to evaluate stratification in the eastern Bering Sea shelf survey for partial least squares analysis. [Color online.]



RMSEP and RMSECV should be similar; however, the accuracy of the NIR calibration model is always dependent upon the accuracy of the reference data that were used to create and validate it. Another statistic used to evaluate the performance of the calibration model is the residual prediction deviation (or RPD). The RPD is equal to the standard deviation of the reference values divided by the prediction error of the calibration model, either the RMSECV or the RMSEP. There are no universal guidelines for determining an acceptable RPD, but in general, a minimum value of 3 is desired.

The assessment of model performance and robustness (ability to predict independent and unobserved samples) is based on the following PLS statistics: (1) coefficient of determination (r^2) of cross calibration (r_c^2) and external validation/prediction (r_v^2), (2) RMSECV and RMSEP: $RMSEP = \sqrt{\frac{1}{M} \sum_{i=1}^M (Y_i^{Meas} - Y_i^{Pred})^2}$, where Y is the age of the i th fish, and M is the number of samples, (3) model bias (B_M) (average difference between predicted and observed values), and (4) slope of the calibration/validation model.

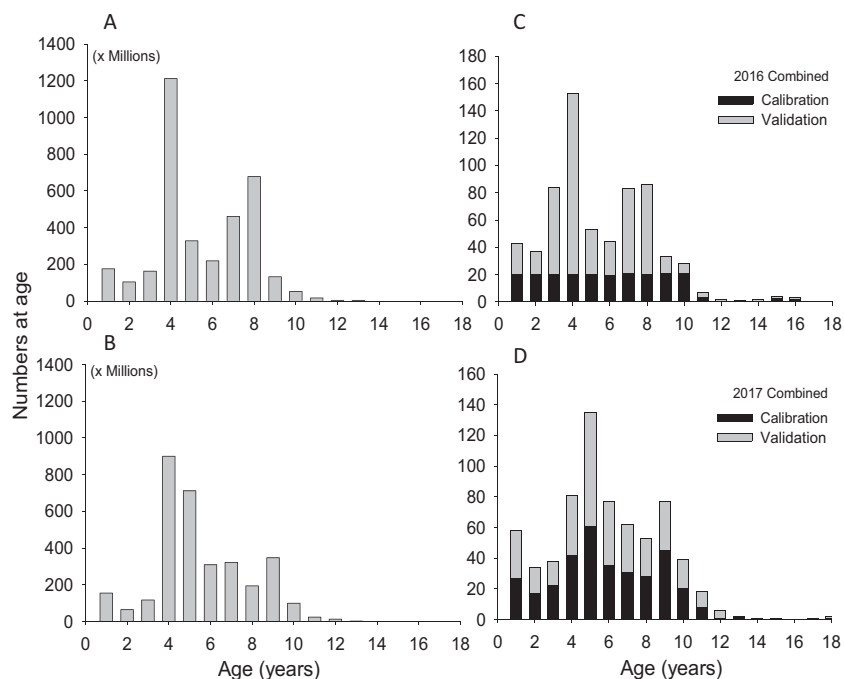
We also assessed the accuracy between ages generated between the FT-NIR and traditional production age estimation procedures by calculating the frequency of the differences as a measure of relative bias ($Bias = B$), $B^{NIR} = (Age^{Prod} - Age^{NIR})$, and $B^{Prod} = (Age^{read} - Age^{test})$.

Results

Walleye pollock condition was spatially related to latitudinal gradient proceeding from high conditions in the southeastern Bering Sea to the northwestern Bering Sea (Fig. 1). Concentrations of generally higher fish condition (>1.0 , a “hotspot”) were clustered between the Aleutian Islands in the south up to Pribilof Islands along the middle and outer depth domains. Above approximately $57^\circ N$ latitude, fish conditions were generally close to or below 1.0 and nonsignificant, and farther to the northwest above $58^\circ N$ latitude, significant concentrations were associated with low-condition (“coldspots”). Hence, in analysis of the 2016 and 2017 FT-NIRS, validation test data were stratified north and south of $57^\circ N$ latitude.

Walleye pollock population age compositions in the 2016 EBS BTS were dominated by relatively large 2012 and 2008 year classes (Fig. 2A). In 2017, the 2012 year class was again prominent as age-5 fish with another 2013 strong year class as age-4 fish (Fig. 2B). Although walleye pollock can grow older than 20 years of age, relatively few fish are captured greater than 12 years of age. Sampling schemes for NIR analysis, while different for 2016 and 2017, were reasonably representative of the population age composition overall (Figs. 2C and 2D). The primary difference is the calibration sample selection; in 2016, otoliths were based on a uniform sampling distribution with target total sample size and in 2017, both calibration and validation samples were the 20% test

Fig. 2. Eastern Bering Sea walleye pollock (*Gadus chalcogrammus*) abundance by age in (A) 2016 and (B) 2017. A large 2012 year class as age-4 fish is evident. Numbers of (C) 2016 and (D) 2017 walleye pollock otoliths selected for FT-NIR analysis in the calibration and validation data sets.



selected at random. Age reading precision from traditional methods was typical of EBS walleye pollock with the PA = 67% (± 0 years), APE = 3.14, and CV = 4.44 in both 2016 and 2017 (Fig. 3). The scatter shows a good correspondence to a 1:1, line indicating little relative bias.

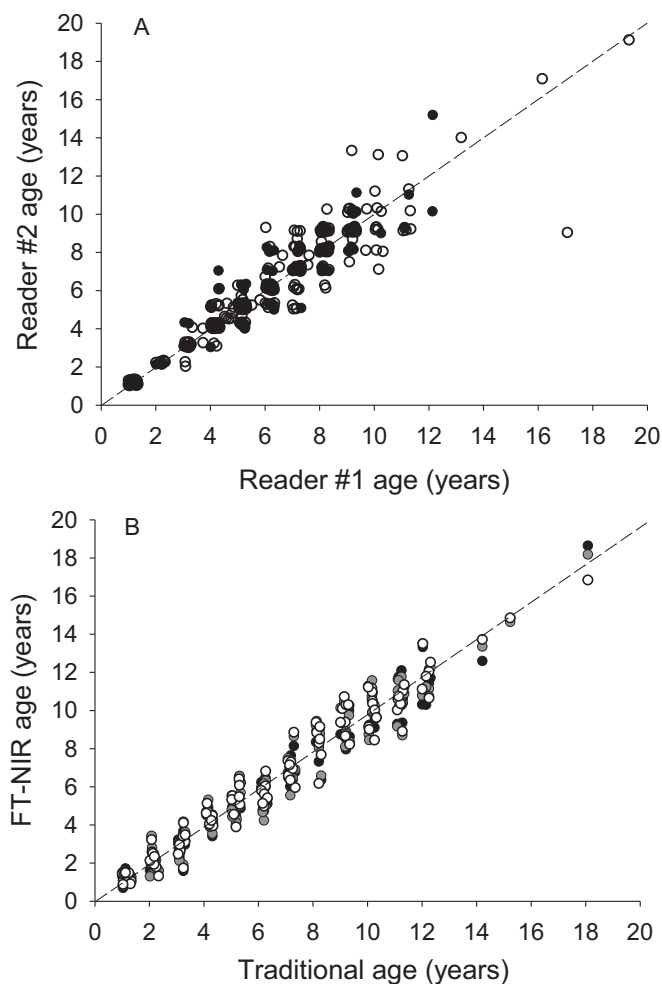
The PLS loadings from the calibration models for 2016, 2017, and 2016–2017 combined were similar for the majority of the wavelength regions, suggesting that similar molecular compounds correlated with traditional ages. The relevant spectral information for all calibration-validation models was isolated primarily in the 6821–5269 and 5022–4171 cm^{-1} spectral regions. Molecular bonds related to these vibrational group frequencies correspond to –CH, –OH, and –NH functional groups. The absorbance spectra for the most informative regions from a selection of 12 walleye pollock otoliths are shown in Fig. 4. Given that the exact nature of molecular species of organic compounds in walleye pollock otoliths is unknown, the characteristic of molecules related to absorbers in the near infrared regions can only be inferred from texts such as that of Workman and Weyer (2008). We did not find statistical differences ($p > 0.10$) in the PLS models with regard to position orientation on the FT-NIR spectrometer stage so future studies could reliably include only a single spectral analysis (Fig. 3). The repeatability of FT-NIR ages from trial to trial was also very good, with the RSD, which is equivalent to the APE, generally below 3.0%, which is shown in Fig. 3 as a tight spread along the 1:1 line.

In total, over 1300 walleye pollock otoliths were scanned for spectral data. Three calibration models were developed ($n = 655$) and their performance evaluated using nine separate external validation data sets ($n = 655$). Calibration models were developed for 2016 and 2017 separately and then 2016–2017 combined (Table 1). Model performance for the 2016 and 2017 calibration models was evaluated from the north and south spectral data. In addition, model performance was evaluated for the 2016–2017 combined calibration model with external validation data from 2016 and 2017 individually and then combined. The 2016, 2017, and 2016–2017 combined calibration models yielded good predictability, producing an $r_c^2 = 0.91$ to 0.95 (Table 1). Calibration models

were qualitatively similar in appearance and had roughly equivalent calibration statistics, so only the 2016–2017 combined PLS calibration model is shown in Fig. 5, although detailed statistics are given in Table 1. Graphically, the calibration shows a tight correspondence to a 1:1 line, indicating exact equality between the predicted FT-NIRS age in the cross validation and the traditional age estimates. Age estimates included in the calibration model ranged from age-1 to age-15 encompassing all age classes observed in the 2016–2017 surveys. Other measures of calibration model fit were favorable as well: RMSECV = 0.78 to 0.97, RPD = 2.99 to 3.85, and very low overall bias = –0.003 to 0.002. In simple terms, this means that in the cross validation, 90% (or better) of the variability in FT-NIRS ages generated from the spectral data in walleye pollock otoliths was explained by ages estimated by analysts using traditional methods. Also, in the cross validation, the predicted FT-NIRS ages from the calibration model were accurate within ± 1 year based on the RMSECV.

In the external validation, the predictive calibration model performance for 2016 and 2017 was better when combining the north and south external validation data (Table 1). The predictive performance measures were $r_v^2 = 0.93$, RMSEP = 0.88 years, and RPD = 3.21 for 2016 and $r_v^2 = 0.91$, RMSEP = 1.04 years, and RPD = 3.09 for 2017 (Table 1). In general, calibration model performance degraded slightly when externally validated with south data where the r_c^2 dropped to $r_v^2 = 0.82$ and 0.85 for 2016 and 2017, respectively. In both cases, the RPD declined below a value of 3.0. When combining 2016 and 2017 spectral data into a single calibration model (Fig. 5A) and validated against each year, performance was also overall good: $r_v^2 = 0.91$ for 2016 and $r_v^2 = 0.88$ for 2017 (Table 1; Figs. 5C and 5D). In each case where data were combined over space and time, the RPD was 3.0 or greater. Model bias was lower than nearly all previous model evaluations in this case (–0.046 and –0.036), probably due to the large increase in spectral data for calibration. RMSEP was 0.817 and 1.12 years for the 2016 and 2017 validation tests, respectively, and indicates that there is only a 0.2 of a year difference in prediction accuracy between years. Hence, the north and south data for both 2016 and 2017 were combined to

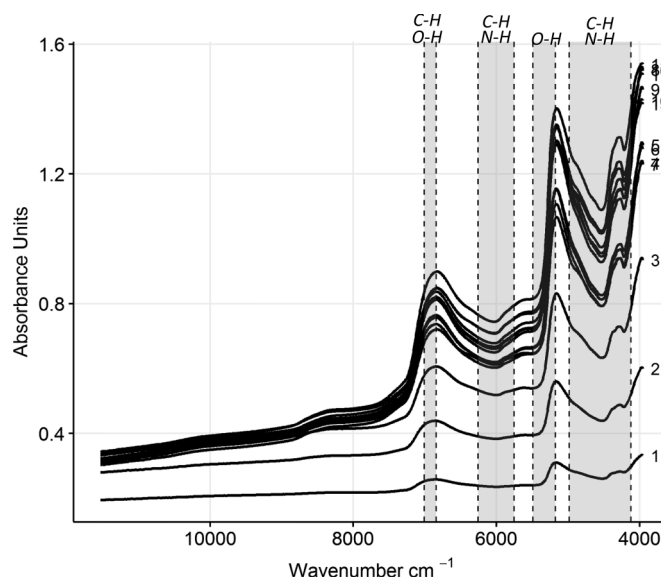
Fig. 3. Walleye pollock (*Gadus chalcogrammus*) ageing precision shown as (A) age-to-age plots from traditional ageing methods for 2016 (open circles) and 2017 (black circles) and (B) triplicate FT-NIR spectroscopy ages associated with a single traditionally estimated age.



develop a global calibration model for EBS walleye pollock representing that spectral variability.

The accuracy (or relative bias) between ages generated between the FT-NIR and traditional production age estimation procedures was evaluated for 2016 and 2017 separately and then for 2016–2017 combined. Qualitatively, there was little difference in relative bias comparisons between the FT-NIR and traditional ageing approaches, so only the combined 2016–2017 analysis is shown in Fig. 6. Frequency histograms of relative bias between the two age determination procedures were nominal. For the 2016–2017 combined data, 75% of the FT-NIR age estimates were the same as traditional production ages, while 68% of the reader and tester ages from the traditional age reading procedure were identical (Fig. 6A). Similarly, 94% and 92% of the FT-NIR and standard ageing procedure, respectively, were the same by ± 1 year of age. Relative bias by age was largely indistinguishable between the ageing procedures up to 10 years of age, after which FT-NIR ages were consistently less biased than the standard production procedure in 2016 (Fig. 6B). Sample numbers diminish rapidly after 10 years of age, so estimates are less reliable. In general, these results suggest that age estimation using FT-NIR spectroscopy of walleye pollock otoliths replicated the traditional age estimation procedure with equal or slightly better precision.

Fig. 4. Selected spectral data for age-1 through age-12 eastern Bering Sea walleye pollock (*Gadus chalcogrammus*) otoliths. Shaded regions of absorbance signatures by wavenumber show molecular vibrational group frequencies most relevant to age estimation from FT-NIR.



Discussion

While FT-NIR spectroscopy has its roots in the manufacturing/industrial sciences, there are numerous examples of the application of NIR spectrometry in ecological and wildlife research in recent years for which Vance et al. (2016) provide citations in both invertebrate and vertebrate studies. The most common application of NIR spectroscopy in vertebrate wildlife ecology, particularly mammals, is the analysis of fecal samples for questions of nutrition, diet composition, and parasitology (Vance et al. 2016). For instance, investigators examined the use of NIR spectroscopy to analyze marine mammal diets via fecal analysis (Kaneko and Lawler 2006). In fisheries ecology research, we found only a few published studies for which NIR spectroscopy has been used to age fish from hard structures. Wedding et al. (2014) aged otoliths from a demersal snapper (*Lutjanus malabaricus*), while Rigby et al. (2014, 2016) aged two shark species (*Sphyrna mokarran* and *Carcharhinus sorrah*) from vertebrae. Two other species of fish, barramundi (*Lates calcarifer*) and snapper (*Pagrus auratus*), have also been analyzed (Robins et al. 2015).

Compared to other studies for fishes, our results for ageing EBS walleye pollock from FT-NIR spectroscopy of otoliths was equally promising. For instance, for saddletail snapper (Wedding et al. 2014), the calibration model yielded $r^2 = 0.93$ and RMSECV of 1.35 with equally good validation statistics (r^2 of 0.94 and RMSECV of 1.54). For the two species of sharks (Rigby et al. 2016), FT-NIR analyses were slightly poorer where calibration models r^2 yielded 0.84–0.89. The three calibration models developed for walleye pollock in this study from over 1500 spectra analyzed yielded r^2 between 0.91 and 0.95 for calibration models (which combined the entire survey area) and nearly equally good external validation statistics ($r^2 = 0.93$ and RMSECV of 0.88 for 2016 and $r^2 = 0.91$ and RMSECV of 1.0). This indicates that walleye pollock age could be predicted within ± 1.0 increment count or year of age about 67% of the time.

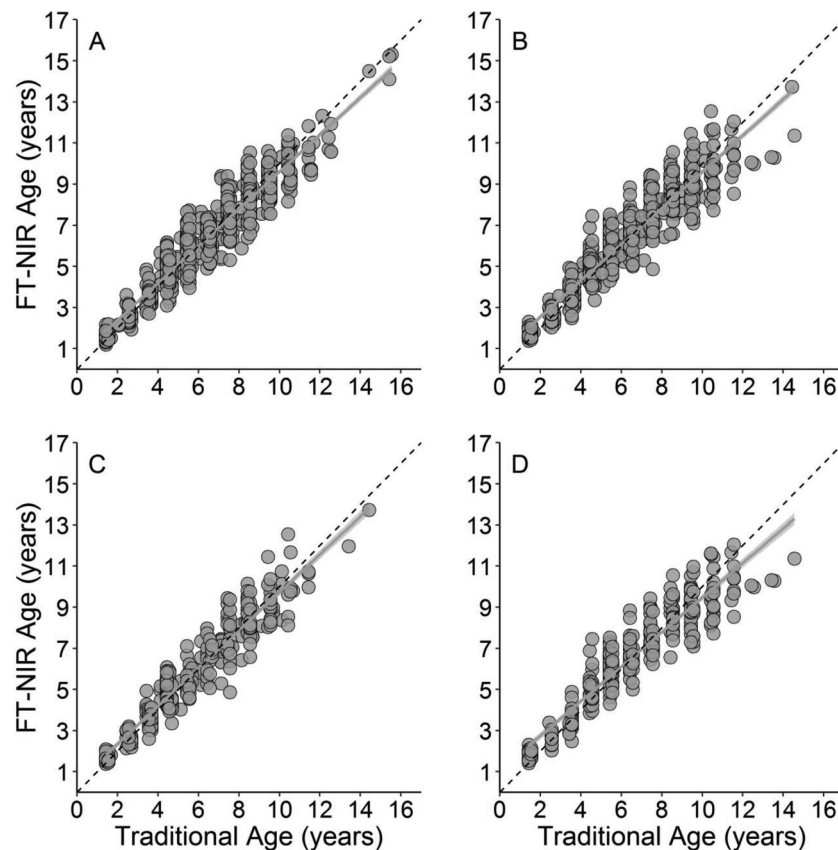
The accuracy of predicting ages from future samples depends on the validity of the calibration models that must be assessed for every species analyzed. The validity of a calibration model will need to be assessed as to how robust model results are to variability in otolith microchemistry, which is thought to be an interaction between fish physiology and environment (Chang and Geffen

Table 1. Results of partial least squares model to eastern Bering Sea walleye pollock (*Gadus chalcogrammus*) showing three calibration and nine validation model statistics.

Calibration	Calibration model statistics							
	r^2	n	RMSECV	RPD	Bias	Slope	Offset	
2016 north and south	94.6	202	0.78	3.85	0.002	0.99	-0.17	
2017 north and south	92.4	340	0.966	2.99	-0.003	0.89	0.69	
2016 and 2017	91.3	654	0.826	3.26	-0.001	0.91	0.56	
Validation set	External validation statistics							
	r^2	n	RMSEP	Bias	SEP	RPD	Offset	Slope
2016 North	0.87	217	0.667	0.187	0.641	4.21	0.44	1.00
2016 South	0.82	232	1.040	-0.551	0.886	2.13	1.65	0.82
2016 North and south	0.93	449	0.882	-0.195	0.860	3.21	0.44	0.96
2017 North	0.89	173	1.090	0.231	1.070	3.21	0.79	0.88
2017 South	0.85	171	0.975	-0.240	0.945	2.31	0.60	0.94
2017 North and south	0.91	344	1.040	-0.004	1.040	3.09	0.69	0.89
2016	0.91	328	0.817	-0.046	0.817	3.28	0.51	0.92
2017	0.88	338	1.120	-0.036	1.120	2.65	1.07	0.84
2016 and 2017	0.89	665	0.957	-0.050	0.956	3.14	0.87	0.86

Note: RMSECV, root mean square error of cross validation; RPD, residual prediction deviation; RMSEP, root mean square error of prediction; SEP, square error of prediction.

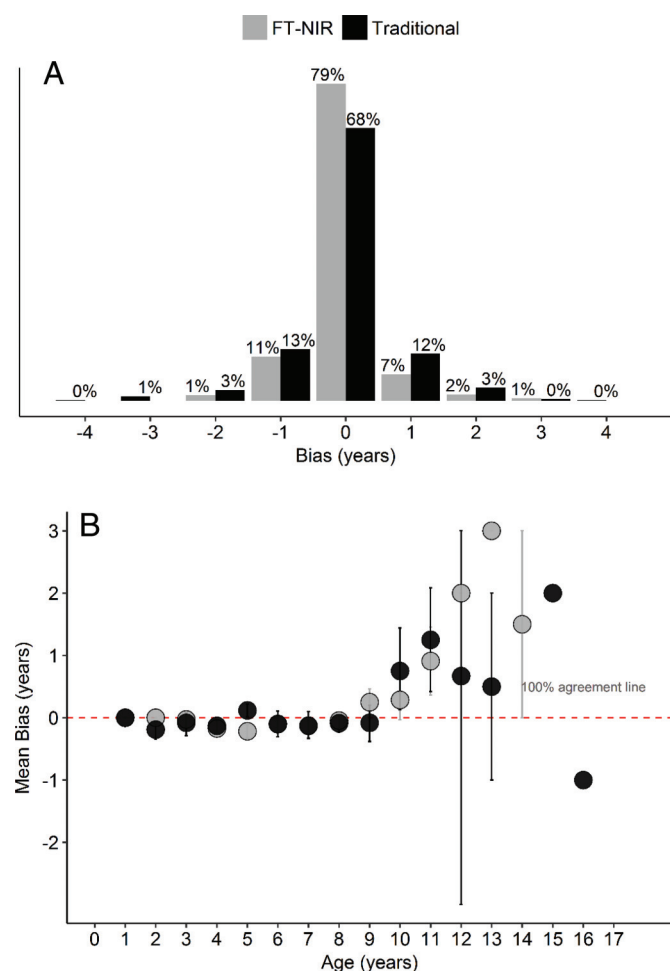
Fig. 5. (A) Calibration model from 2016–2017 combined eastern Bering Sea walleye pollock (*Gadus chalcogrammus*) otoliths showing predicted of FT-NIR spectroscopy ages from traditional age estimation. External validation of calibration model performance is shown for (B) 2016–2017 data combined and from (C) 2016 and (D) 2017 data separately.



2013). Ontogenetic changes of fish related to growth rate, reproduction, feeding, diet changes, and stress are known to influence trace element assimilation in otoliths (Radtke and Shafer 1992). Furthermore, the chemical composition of the water varies geographically and over time, so environmental factors such as depth, salinity, and temperature will also play a role (Chang and Geffen 2013). Wedding et al. (2014) found that conditions in otolith microchemistry were so variable between post-wet and post-dry

seasons for saddletail snapper that calibration models were not robust across seasons but recommended combining the data to account for this variability. In another study of geographic variability, Robins et al. (2015) found calibration models for a specific location and season are not as successful at predicting age across at differing locations or seasons for the river species of barramundi or coastal snapper. This highlights the fact that there is much to be learned regarding the biological and physical factors

Fig. 6. Comparison of accuracy between ages generated between the FT-NIR and traditional age estimation procedures by calculating the frequency of the differences (Bias = B), $B^{FT-NIR} = (Age^{Trad} - Age^{FT-NIR})$, and $B^{Trad} = (Age^{read1} - Age^{read2})$. (A) Frequency of bias over all ages and (B) mean bias by age. [Color online.]



contributing to spectral variability in fish otoliths. Insight from other disciplines using FT-NIR would suggest that prediction accuracy becomes less sensitive to unknown factors when more variability is accounted for (Bobelyn et al. 2010). However, too much biological variability may lead to greater prediction uncertainty limiting the utility of the approach for age estimation.

In most research applications, knowledge of water chemistry and precise biological factors affecting the molecular constituents activated by NIR will not be known, so efforts to evaluate model robustness might consider broad-scale geographic and temporal factors. We spatially stratified the 2016 and 2017 EBS otolith samples on the basis of walleye pollock body condition to evaluate model robustness but found only a nominal difference between the north and south in 2016 (RMSEP was 33% higher in the south compared to the north). Where the south otoliths were incorporated into the 2016 and 2017 validation, the RPD fell 35% and 13%, respectively. The extent to which the otoliths from the south affected the model performance each year is unclear; however, the presence of the very large 2012 year class, most of which occurred in the south, may be influencing the results (i.e., over-prediction of FT-NIR ages for 2016 south validation). Subsequent analysis of 2016 samples where associated otolith masses were considered revealed that larger model residuals were related ($r = 0.5, p < 0.001$) to heavier otolith masses at age 4. This may suggest that some otoliths estimated to be age 4 by the traditional meth-

ods had an otolith mass more consistent with age-5 walleye pollock. Error in age assignment of fish to a particularly large cohort when present in the population age composition has been identified as a source of ageing error (Kimura et al. 1992). Nevertheless, model robustness was still very promising when combining 2016 and 2017, as well as two survey years' data, over the entire survey area, which seemed to account for the unequal distribution of the dominant age-4 fish in the EBS. We suggest that future study examine cohort effects on the prediction accuracy and variability they impart to the spectral data. Effects on otolith spectra are likely a combination of both biologically intrinsic and environmentally extrinsic factors. A principal component analysis, for instance, may reveal whether fish age or year of growth has more spectral variation in otolith samples, but such an analysis would require many more years of otolith spectra.

Prediction accuracy of FT-NIR ages will only be as good as the accuracy in the calibration samples that are provided, and whenever possible, an age validation (estimation of true ageing bias) should be conducted to facilitate the use of FT-NIR age estimation. EBS walleye pollock ages are not without error nor has the age determination method used been unequivocally validated. From over hundreds of thousands of historic walleye pollock double readings, the ageing precision at AFSC has been well characterized and the FT-NIR ageing process has replicated this quite well. However, the impact of that observation error on the FT-NIR model calibration results needs further investigation. In terms of ageing (true) bias, the general age range and longevity of walleye pollock have been determined from Pb/Ra studies (Kastelle and Kimura 2006); they found an average of a 0.8 year bias between Pb/Ra ages and traditional ages. Also, recent work (C. Kastelle, unpublished) using $\Delta^{14}C$ indicates that ageing bias using traditional methods is within the accuracy of at least ± 1 -3 years, which is the limit of resolution associated with that technique (Campana 1999). Other measures of ageing bias, such as known age fish, are not available for walleye pollock (Kastelle and Kimura 2006). Therefore, it is quite possible that age misassignment by 1 year less than the true age (i.e., misassigning age 5 fish to age 4) may have resulted in observation error rather than prediction error in some cases, particularly in the south data, which had an effect on calibration. Efforts to derive true walleye pollock ages will only improve the calibration model and age validation studies should be undertaken to reduce prediction bias.

Precision and efficiency is one of the main benefits of FT-NIR age estimation procedures over traditional approaches. Age determination precision using the FT-NIR spectroscopy was as good as, or better than, the traditional ageing methods. Generally, we found a slightly greater percentage of the sample in agreement between the FT-NIR age and the reference age than between two independent age reading analysts. Also relative bias by age was as good or slightly better using FT-NIR up to, in most cases, 12 years of age, which represents the vast majority of population numbers (Ianneli et al. 2017). One reason for possibly better precision with FT-NIR is that traditional age determination methods of growth zone counts are inherently a subjective process of pattern recognition between two people (Campana 1999). Many factors are at play that can result in a discrepancy in the age estimates between analysts (even assuming use of a standardized age determination criteria) including variation in sample processing, sample presentation, and microscopic errors as well as personal well-being and stress. Most production ageing laboratories apply rigorous quality control measures to maintain consistency and guard against relative bias. By its nature, FT-NIR spectroscopy is a quantitative technique (once the parameters for scanning and wavenumber ranges are selected) that measures the vibrational frequencies of covalent bonds in the otolith molecules. Since the instrument is frequently internally calibrated, the spectral data are acquired with high repeatability (Roggio et al. 2007). With a robust model, efficiency is one of the major benefits of FT-NIR over traditional

production ageing procedures. Samples can be analyzed whole without labor-intensive sample processing such as embedding in resin, sectioning, cutting, roasting, etc., and final microscopic examination. We estimate that, on average, it takes an age reading analyst approximately 3–5 min to estimate a single fish age using traditional procedures compared to approximately 50 s to estimate an age from a walleye pollock otolith using FT-NIR spectroscopy. Thus, once an initial set of 120 otoliths were scanned for spectral data, age was estimated using traditional methods and the model calibrated; FT-NIR had the capacity to generate 360 ages per day compared to 35 ages per day (based on 6 h actively age reading). The use of FT-NIR spectroscopy for the rapid assessment of fish ages from otoliths, either in the laboratory or on ship-board research surveys, could be transformative for providing a key data source for stock assessments and ultimately management advice. The large number of spectra collected and favorable results reported from this study indicate that operationalizing the age production process for EBS walleye pollock stock assessments is feasible and developing protocols for implementation is the next step.

Acknowledgements

We thank Betty Goetz, Jeremy Harris, Chris Gburski, and Charlie Piston of the Alaska Fisheries Science Center (AFSC) Age and Growth Laboratory with assistance with microscopic ageing of walleye pollock otoliths. Jim Ianelli and Martin Dorn, also from AFSC, provided a thorough review of early drafts for this manuscript. We also thank the anonymous reviewers for insightful comments to improve the manuscript. The findings and conclusions in the paper of those of the author(s) and do not necessarily represent the views of the National Marine Fisheries Service. Reference to trade names does not imply endorsement by the National Marine Fisheries Service, NOAA.

References

Bagenal, T., and Tesch, F. 1978. Age and growth in method of assessment of fish production in fresh water. IBP Handbook. Blackwell Scientific Press, Oxford.

Beamish, R., and Fournier, D. 1981. A method for comparing the precision of a set of age determinations. *Can. J. Fish. Aquat. Sci.* **38**(8): 982–983. doi:10.1139/f81-132.

Beamish, R., and McFarlane, G.A. 1995. A discussion of the importance of aging errors, and an application to walleye pollock: the world's largest fishery. In *Recent developments in fish otolith research*. University of South Carolina Press, Columbia. pp. 545–566.

Begg, G.A., Campana, S.E., Fowler, A.J., and Suthers, I.M. 2005. Otolith research and application: current directions in innovation and implementation. *Mar. Freshw. Res.* **56**: 477–483. doi:10.1071/MF05111.

Bertignac, M., and De Pontual, H. 2007. Consequences of bias in age estimation on assessment of the northern stock of European hake (*Merluccius merluccius*) and on management advice. *ICES J. Mar. Sci.* **64**: 981–988. doi:10.1093/icesjms/fsm039.

Bobelyn, E., Serban, A.-S., Nicu, M., Lammertyn, J., Nicolai, B.M., and Saeys, W. 2010. Postharvest quality of apple predicted by NIR-spectroscopy: study of the effect of biological variability on spectra and model performance. *Postharvest Biol. Technol.* **55**: 133–143. doi:10.1016/j.postharvbio.2009.09.006.

Campana, S.E. 1999. Chemistry and composition of fish otoliths: pathways, mechanisms and applications. *Mar. Ecol. Prog. Ser.* **188**: 263–297. doi:10.3354/meps188263.

Campana, S.E., and Thorrold, S.R. 2001. Otoliths, increments, and elements: keys to a comprehensive understanding of fish populations? *Can. J. Fish. Aquat. Sci.* **58**(1): 30–38. doi:10.1139/f00-177.

Chang, M.-Y., and Geffen, A.J. 2013. Taxonomic and geographic influences on fish otolith microchemistry. *Fish. Fish.* **14**: 458–492. doi:10.1111/j.1467-2979.2012.00482.x.

Chang, W.Y. 1982. A statistical method for evaluating the reproducibility of age determination. *Can. J. Fish. Aquat. Sci.* **39**(8): 1208–1210. doi:10.1139/f82-158.

Chen, J., and Wang, X.Z. 2001. A new approach to near-infrared spectral data analysis using independent component analysis. *J. Chem. Inf. Comput. Sci.* **41**: 992–1001. doi:10.1021/ci0004053. PMID:11500115.

Chen, Y., Chen, L., and Stergiou, K.I. 2003. Impacts of data quantity on fisheries stock assessment. *Aquat. Sci.* **65**: 92–98.

Chilton, D.E., and Beamish, R.J. 1982. Age determination methods for fishes studied by the Groundfish Program at the Pacific Biological Station. *Can. Spec. Publ. Fish. Aquat. Sci.* **60**.

Coggins, L.G., Jr., Gwinn, D.C., and Allen, M.S. 2013. Evaluation of age-length key

sample sizes required to estimate fish total mortality and growth. *Trans. Am. Fish. Soc.* **142**: 832–840. doi:10.1080/00028487.2013.768550.

Conn, P.B., Williams, E.H., and Shertzer, K.W. 2010. When can we reliably estimate the productivity of fish stocks? *Can. J. Fish. Aquat. Sci.* **67**(3): 511–523. doi:10.1139/F09-194.

Conner, J., and Lauth, R.R. 2017. Results of the 2016 eastern Bering Sea continental shelf bottom trawl survey of groundfish and invertebrate resources. U.S. Dep. Commer. NOAA Tech. Memo. NMFS-AFSC-352.

De Pontual, H., Groison, A.L., Piñeiro, C., and Bertignac, M. 2006. Evidence of underestimation of European hake growth in the Bay of Biscay, and its relationship with bias in the agreed method of age estimation. *ICES J. Mar. Sci.* **63**: 1674–1681. doi:10.1016/j.icesjms.2006.07.007.

Fablet, R., and Le Josse, N. 2005. Automated fish age estimation from otolith images using statistical learning. *Fish. Res.* **72**(2–3): 279–290. doi:10.1016/j.fishres.2004.10.008.

Fablet, R., Chessel, A., Carbini, S., Benzinou, A., and de Pontual, H. 2009. Reconstructing individual shape histories of fish otoliths: a new image-based tool for otolith growth analysis and modeling. *Fish. Res.* **96**(2–3): 148–159. doi:10.1016/j.fishres.2008.10.011.

Getis, A., and Ord, J.K. 1992. Analysis of spatial association by use of distance statistics. *Geogr. Anal.* **24**(3): 189–206. doi:10.1111/j.1538-4632.1992.tb00261.x.

Hilborn, R., and Walters, C.J. 1992. Quantitative fisheries stock assessment: choice, dynamics and uncertainty. *Rev. Fish Biol. Fish.* **2**: 177–178. doi:10.1007/BF00042883.

Ianelli, J., Kotwicki, S., Honkalehto, T., Hoslmán, K., and Fissel, B. 2017. Assessment of the walleye pollock stock in the eastern Bering Sea. In *Stock assessment and fishery evaluation report for the groundfish resources of the Bering Sea/Aleutian Islands regions*. North Pacific Fishery Management Council, Anchorage, Alaska.

Kaneko, H., and Lawler, I.R. 2006. Can near infrared spectroscopy be used to improve assessment of marine mammal diets via fecal analysis? *Mar. Mammal Sci.* **22**: 261–275. doi:10.1111/j.1748-7692.2006.00030.x.

Kastelle, C.R., and Kimura, D.K. 2006. Age validation of walleye pollock (*Theragra chalcogramma*) from the Gulf of Alaska using the disequilibrium of Pb-210 and Ra-226. *ICES J. Mar. Sci.* **63**(8): 1520–1529. doi:10.1016/j.icesjms.2006.06.002.

Kimura, D.K., and Anderl, D.M. 2005. Quality control of age data at the Alaska Fisheries Science Center. *Mar. Freshw. Res.* **56**(5): 783–789. doi:10.1071/MF04141.

Kimura, D., Lyons, J., MacLellan, S., and Goetz, B. 1992. Effects of year-class strength on age determination. *Mar. Freshw. Res.* **43**: 1221–1228. doi:10.1071/MF9921221.

Mahe, K., Rabhi, K., Bellamy, E., Elleboode, R., Aumond, Y., Huet, J., Cresson, P., and Roos, D. 2016. Growth of the oblique-banded grouper (*Epinephelus radiatus*) on the coasts of Reunion Island (SW Indian Ocean). *Cybiurn*, **40**(1): 61–65.

Matta, M.E., and Kimura, D.K. (Editors). 2012. Age determination manual of the Alaska Fisheries Science Center Age and Growth Program. U.S. Dep. Commer. NOAA Professional Paper NMFS 13.

Maudner, M.N., and Punt, A.E. 2013. A review of integrated analysis in fisheries stock assessment. *Fish. Res.* **142**: 61–74. doi:10.1016/j.fishres.2012.07.025.

Nasreddine, K., Benzinou, A., and Fablet, R. 2013. Geodesics-based image registration: applications to biological and medical images depicting concentric ring patterns. *IEEE Trans. Image Process.* **22**(11): 4436–4446. doi:10.1109/TIP.2013.2273670.

Ono, K., Licandeo, R., Muradian, M.L., Cunningham, C.J., Anderson, S.C., Hurtado-Ferro, F., Johnson, K.F., McGilliard, C.R., Monnahan, C.C., Suwalski, C.S., Valero, J.L., Vert-Pre, K.A., Whitten, A.R., and Punt, A.E. 2015. The importance of length and age composition data in statistical age-structured models for marine species. *ICES J. Mar. Sci.* **72**: 31–43. doi:10.1093/icesjms/fsu007.

Pilling, G.M., Millner, R.S., Easey, M.W., Maxwell, D.L., and Tidd, A.N. 2007. Phenology and North Sea cod *Gadus morhua* L.: has climate change affected otolith annulus formation and growth? *J. Fish Biol.* **70**(2): 584–599. doi:10.1111/j.1095-8649.2007.01331.x.

Radtke, R.L., and Shafer, D.J. 1992. Environmental sensitivity of fish otolith microchemistry. *Mar. Freshw. Res.* **43**: 935–951. doi:10.1071/MF9920935.

Reeves, S.A. 2003. A simulation study of the implications of age-reading errors for stock assessment and management advice. *ICES J. Mar. Sci.* **60**: 314–328. doi:10.1016/S1054-3139(03)00011-0.

Ricker, W.E. 1975. Computation and interpretation of biological statistics of fish populations. *Dep. Environ. Fish. Mar. Serv. Bull.* **191**.

Rigby, C.L., Wedding, B.B., Grauf, S., and Simpfendorfer, C.A. 2014. The utility of near infrared spectroscopy for age estimation of deepwater sharks. *Deep-Sea Res. Part I Oceanogr. Res. Pap.* **94**: 184–194. doi:10.1016/j.dsr.2014.09.004.

Rigby, C.L., Wedding, B.B., Grauf, S., and Simpfendorfer, C.A. 2016. Novel method for shark age estimation using near infrared spectroscopy. *Mar. Freshw. Res.* **67**(5): 537–545. doi:10.1071/MF15104.

Robins, J.B., Wedding, B.B., Wright, C., Grauf, S., Sellin, M., Fowler, A., Saunders, T., and Newman, S. 2015. Revolutionising fish ageing: using near infrared spectroscopy to age fish. Department of Agriculture, Fisheries and Forestry, Brisbane, April 2015. CC BY 3.0. <http://www.frdc.com.au/Archived-Reports/FRDC%20Projects/2012-011-DLD.pdf>.

Roggo, Y., Chalup, P., Maurer, L., Lema-Martinez, C., Edmond, A., and Jent, N. 2007. A review of near infrared spectroscopy and chemometrics in pharma-

- ceutical technologies. *J. Pharma. Biomed. Anal.* **44**: 683–700. doi:10.1016/j.jpba.2007.03.023.
- Stauffer, G. (Compiler). 2004. NOAA protocols for groundfish bottom trawl surveys of the nation's fishery resources. U.S. Dep. Commer. NOAA Tech. Memo. NMFS-F/SPO-65 (.pdf, 563MB). <http://spo.nmfs.noaa.gov/tm/tm65.pdf>.
- Troade, H., and Benzinou, A. 2002. Computer assisted age estimation. In *Manual of fish sclerochronology*. Edited by J. Panfili, H. de Pontual, H. Troade, and P.J. Wright. Ifremer-IRD coedition, Brest, France. pp. 199–241.
- Vance, C.K., Tolleson, D.R., Kinoshita, K., Rodriguez, J., and Foley, W.J. 2016. Near infrared spectroscopy in wildlife and biodiversity. *J. Near Infrared Spectros.* **24**: 1–25. doi:10.1255/jnirs.1199.
- Wedding, B.B., Forrest, A.J., Wright, C., Grauf, S., and Exley, P. 2014. A novel method for the age estimation of saddletail snapper (*Lutjanus malabaricus*) using Fourier transform – near infrared (FT-NIR) spectroscopy. *Mar. Freshw. Res.* **65**: 894–900. doi:10.1071/MF13244.
- Workman, J., and Weyer, L. 2008. *Practical guide to interpretive near-infrared spectroscopy*. CRC Press Taylor & Francis Group, Boca Raton, Fla.
- Zorica, B., Sinovic, G., and Kec, V.C. 2010. Preliminary data on the study of otolith morphology of five pelagic fish species from the Adriatic Sea (Croatia). *Acta Adriatica*, **51**: 89–96.